Toughening Hydrogels Through Force-triggered Chemical Reactions that Lengthen Polymer Strands

Authors: Zi Wang[1,2], Xujun Zheng[1], Tetsu Ouchi[1,2], Tatiana B. Kouznetsova[1,2], Haley K. Beech[2,5], Sarah Av-Ron[5], Takahiro Matsuda[7], Brandon H. Bowser[1,2], Shu Wang[1,2], Jeremiah A. Johnson[2,3*], Julia A. Kalow[2,4*], Bradley D. Olsen[2,5*], Jian Ping Gong[2,6,7,8*], Michael Rubinstein[1,2,6,8,9*], and Stephen L. Craig[1,2,6*]

Affiliations:

[1]Department of Chemistry, Duke University, Durham, NC, USA 27708-0346

[2]NSF Center for the Chemistry of Molecularly Optimized Networks

[3]Department of Chemistry, MIT, Boston, MA, USA

[4]Department of Chemistry, Northwestern University, Evanston, IL, USA

[5]Department of Chemical Engineering, MIT, Boston, MA, USA

[6]Soft Matter GI-CoRE, Hokkaido University, N21W11, Kita-ku, Sapporo 001-0021, Japan

[7]Faculty of Advanced Life Science, Hokkaido University, N21W11, Kita-ku, Sapporo 001-0021, Japan

[8]Institute for Chemical Reaction Design and Discovery (WPI-ICReDD), Hokkaido University, N21W11, Kita-ku, Sapporo 001-0021, Japan

[9]Department of Mechanical Engineering and Materials Science, Biomedical Engineering, and Physics, Duke University, Durham, NC, USA

*Correspondence to: jkalow@northwestern.edu, jaj2109@mit.edu, bdolsen@mit.edu, gong@sci.hokudai.ac.jp, michael.rubinstein@duke.edu, stephen.craig@duke.edu

Abstract: The utility and lifetime of materials made from polymer networks, including hydrogels, depend on their capacity to stretch and resist tearing. In gels and elastomers, those mechanical properties are often limited by the covalent chemical structure of the polymer strands between cross-links, which is typically fixed during the material synthesis. We report polymer networks in which the constituent strands lengthen through force-coupled reactions that are triggered as the strands reach their nominal breaking point. In comparison to networks made from analogous control strands, reactive strand extensions of up to 40% lead to hydrogels that stretch 40-50% further and exhibit tear energies that are twice as large. The enhancements are synergistic with those provided by double network architectures, and complement other existing toughening strategies.

One Sentence Summary: Polymer strands that react to grow longer upon stretching lead to improved extensibility and tear resistance in hydrogels.

Main Text:

The physical breakdown of polymeric materials such as elastomers and hydrogels occurs during periods of mechanical strain (*1, 2*), and it limits their useful scope and lifetime. This has resulted in strategies that improve the durability of polymer networks (*3*), including the use of multi-network architectures (*3, 4*), reversible cross-linking, noncovalent domain unfolding (*5*), and the addition of fillers (*6*). All these approaches have in common that the primary, covalent chemical structure of the network remains fixed up until the point that the polymer strand breaks.

Polymer networks that actively remodel their primary, covalent structure during use therefore have the potential to provide property enhancements that complement existing mechanisms. Recent advances in covalent polymer mechanochemistry now enable the synthesis of polymer strands that extend the covalent bonding along their backbone when stretched (*7*), as a result of force-coupled chemical reactions that are triggered at or just before the strands reach their nominal breaking point. Because these reactions are typically associated with high forces (~nN), the amount of energy absorbed at the single molecular level can be quite large relative to the energy absorbed by a covalent strand in the absence of the reaction-enabled extension (*8*). Existing models of network fracture draw a direct relationship between the energy required to propagate a crack through a rubbery material (the tear energy, *T*) and the energy required to stretch an individual polymer strand to the point at which it breaks (the chain fracture energy, *U*) (*9*). We therefore hypothesized that by turning a polymer network into a literal network of responsive chemical reactions, reactive strand extension might improve the properties of an existing bulk material.

The RSE concept is shown in Fig. 1. Strand extension is provided by the sodium salts of bicyclo[6.2.0]decane (BCD) mechanophores (Fig. S1), which react via a force-coupled [2+2] cycloreversion to release stored length (*10*). BCD co-polymers are formed via the radical addition co-polymerization of the corresponding bicyclic cyclobutene carboxylate monomer **1a**. Mechanophore reactivity was quantified using single-molecule force spectroscopy (SMFS) implemented through an atomic force microscope (AFM). Co-polymerization of **1a** with 2-acrylamido-2-methylpropane sulfonate (NaAMPS) **2** and acetoacetate methacrylate **3** (for strong attachments) provided linear co-polymers **P1** with **1a**:**2**:**3** = 0.22:0.62:0.16. At forces of up to ~1500 pN, the SMFS curves are typical of a flexible polymer strand overcoming conformational entropy (order of 1 – 10 pN) to reach end-to-end distances that approach its fully extended contour length (order of 10^2 pN). Subsequent stretching is dominated by the deformation of bond angles and bond lengths, as the polymer nears its physical stretching limits before breaking (order of 10^3 pN). With the BCD mechanophore, however, the force-separation curve shows a reproducible release of stored length of up to ~40% of the initial polymer contour length at 1500-2000 pN. This transition is consistent with that expected from the BCD cycloreversion, and the transition force is similar to that reported in other cyclobutane mechanophores (*11*). Pre-extension curves of **P1** overlap well with a those of control strands **P2** made from **1b** (no fused ring, see Fig. S2 for multiple pulls of **P2**), and simulated pulling calculations (see Fig. S3) confirm that the details of scission for the fused and unfused cyclobutanes are effectively indistinguishable. As the polymer strands reach their nominal stretching limit, the presence of selective mechanophores converts strand scission events into force-coupled covalent rearrangements that allow the strands to survive forces and extensions that would otherwise be catastrophic.

The mechanochemically active co-polymers were incorporated into double-network (DN) hydrogels, whose robust mechanical properties facilitate the characterization of mechanical response. DNs consist of two interpenetrating networks with contrasting structure: the first network comprises strands in a highly stretched state and is rigid and brittle. The second network comprises strands in a coiled state, and as a result it is soft and stretchable (*12*). This double-network structure allows multiple strands within the first brittle network to break independently without causing catastrophic breakdown of the entire brittle network, as the local strain amplification created by the breaking of the brittle strand is suppressed by transferring the load to the soft network strands nearby rather than propagating through the first network (*12*). Hydrophilic polymer networks were made via the radical addition co-polymerization of **1a**, NaAMPS **2** (feed concentrations of 0.3 M and 0.7 M, respectively) and *N*,*N'*-methylenebisacrylamide (MBAA) cross-linker. In the DNs, this BCD-AMPS first network was swollen in a precursor solution of acrylamide (AAm, 4 M; MBAA, 0.01 mol%) that was polymerized to form an interwoven, sparsely cross-linked, and highly stretchable polyacrylamide (PAAm) second network (see Fig. S4). Two first networks, **N1** and **N2**, of the same BCD-AMPS content (BCD : AMPS = 3 : 17 mol/mol, see ESI; ~ 40% contour length increase expected from calculations, see Fig. S3) but different cross-linking density (8 mol% and 4 mol% of MBAA for **N1** and **N2**, respectively), were prepared (see Table S1 and Fig. S4).

Control networks **N1-con** and **N2-con** were synthesized using acyclic cyclobutene carboxylate **1b**. The structural similarity of **1a** and **1b** leads to similar reactivity in the polymerization (see Fig. S5), and the similar network structure in **N1** and **N1-con**, or in **N2** and **N2-con**, was verified through equilibrium swelling ratios (V/V_0) of **N1** (12.4 ± 0.1) and **N2** (32.7 ± 0.7) in water that are indistinguishable from those of **N1-con** (12.1 ± 0.9) and **N2-con** (32.7 ± 1.8), respectively, and a gel permeation chromatograph (GPC) comparison of the disassembly products of the first networks (Fig. S6). These single networks were too brittle for reliable mechanical characterization, but the moduli of **DN1** (288 ± 4 kPa) and **DN1-con** (290 ± 8 kPa) fall within experimental uncertainty, as do those of **DN2** (243 ± 5 kPa) and **DN2-con** (249 ± 13 kPa). Thus, any differences in ultimate stretch and tear resistance between the active and control networks are attributed to the conversion of scission to molecular extension and higher breaking force that is allowed in the BCD co-polymers by virtue of the designed release of length stored in the bicyclic ring structure.

The incorporation of the BCD mechanophore leads to substantial changes in the mechanical limits of its double networks. The resistance to tearing was evaluated by introducing a notch into DN films and measuring the strain necessary for the notch to propagate under pure shear loading. Fig. 3A, B shows deformations of notched **DN1** and **DN1-con** under uniaxial extension (see Fig. S7 for stress-strain curves). The critical stretch for crack propagation in **DN1** is 234 ± 4%, which is 40% greater than the 167 ± 7% observed in **DN1-con**. The gain in stretchability is found as well in **DN2**, for which the critical stretch for crack propagation is 128 ± 8%, vs. 83 ± 2% in **DN2-con**. The resistance to tearing can be further quantified in terms of the tear energy *T*, or the energy required per area of crack growth, which was determined via the method of Rivlin and Thomas (*13*). Fig. 3D shows that both **DN1** and **DN2** have roughly double the *T* of their respective controls: 2,840 ± 103 J/m^2 vs. 1,419 ± 52 J/m^2 for **DN1** vs. **DN1-con**, and 554 ± 40 J/m^2 vs. 276 ± 10 J/m^2 for **DN2** vs. **DN2-con**.

The improved mechanical properties due to reactive strand extension are also observed in unnotched **DN1** relative to **DN1-con** (ultimate stretch of 890 ± 120% and 479 ± 99% before breaking, respectively; Fig. 3C and Fig. S8). Notably, **DN1** shows a clear yielding, suggesting that the first network ruptures into a global discontinuous phase that enables the load to be transferred to the second network in the yielded region (*12, 14*). On the other hand, **DN1-con** shows a gradual increase in stress without a clear plateau stress region, suggesting that the internal rupture of the first network is relatively random and does not achieve a global discontinuous structure up to sample failure. We attribute this to the fact that fracture of **N1-con** within **DN1-con** begins at lower strain than **N1**. When a small defect forms, that stress largely remains in **N1-con**, because the second network is still too soft for stress transfer (the local strain at the defect is not great enough). Thus, the fracture propagates further across **N1-con** within the DN and only begins to transfer to the second network after the defect becomes larger. In **DN1**, fracture of **N1** initiates at higher strain, at which point a greater fraction of the stress is transferred to the second network, and so the fracture event is blunted and the next fracture occurs elsewhere, leading to the desired fractal/domain patterns for greater toughness (*12*).

The presence of RSE should alter the energy dissipation behavior from that observed in conventional DN hydrogels. The two systems (e.g., **DN1** vs. **DN1-con**) start with strands that, as seen in the SMFS experiments (Fig. 2B), are effectively identical elastically. In **DN1-con**, a given strand breaks upon reaching a critical strain. In **DN1**, the analogous RSE strand requires the same energy up to that point, but instead of breaking starts to grow longer. This molecular picture leads to two expectations. First, each strand's contribution to the elastic modulus is a function of the ratio of its initial (relaxed) end-to-end distance to final contour length (*15*). Activation of RSE preserves the initial end-to-end distance but increases the final contour length, and RSE therefore reduces a strand's contribution to the tensile modulus, but that reduction is not as great as in the comparison strand that has broken. Therefore, we expect a smaller decrease in modulus with strain under cyclic loading in **DN1** than in **DN1-con**. Second, by the time the RSE strand fully breaks, it will have absorbed and dissipated more energy than the analogous strand that broke without RSE. In other words, we also expect that the RSE strands (**DN1**) will dissipate greater energy per loss of modulus than their non-RSE controls (**DN1-con**).

The expected effects are observed in sequential tensile loading/unloading cycles, where the maximum strain increases from one cycle to the next. When a DN gel is stretched to a given strain for the first time and then unloaded, there is significant hysteresis (*16*) (Fig. 3E; low strain behavior expanded in Fig. 4A, B). Typically, hysteresis in DN gels is attributed almost entirely to chain scission in the first network (*12*) and is correlated with a decrease in modulus due to the loss of stress-bearing network strands (*17*) (Fig. S9 and Fig. S10). Longer elastically effective strands in the first network result in less modulus loss at a given strain (*16, 18*). The initial strand lengths in **DN1** and **DN1-con** are indistinguishable, but RSE in **DN1** suppresses the loss in modulus as expected; greater stretch is required to trigger a measurable change in modulus in **DN1** than **DN1-con**, and the loss in modulus in **DN1** consistently lags that observed in **DN1-con** as a function of strain (Fig. 4C). Further, as seen in Fig. 4D, **DN1** exhibits greater hysteresis per loss in modulus than **DN1-con**, consistent with the ability of RSE to dissipate energy without chain scission.

The concept of reactive chain extension demonstrated here has numerous implications for network design. First, reactive chain extension occurs only at large strains and only at the specific molecular locations that are about to break without it. Unlike the incorporation of weak, reversible cross-linking or noncovalent interstrand interactions, the enhancement does not come with a concomitant increase in the viscous modulus of the network (as evidenced by overlap of repeated unloading/loading cycles at the same maximum strain, see Fig. S11). In other words, the energy dissipation is triggered only when needed to resist fracture and need not be overcome in routine functions of the material when fracture is not imminent. Second, the property enhancements are achieved within networks that otherwise have identical structure and modulus to their non-mechanophore controls, meaning that reactive chain extension might be introduced into at least some materials whose properties are already optimized for a given function, including optimizing the ratio of first and second network swelling to achieve maximum dissipation (*12, 14*). Relative to control DN gels, RSE provides fracture resistance while also suppressing the loss in modulus that accompanies energy dissipation. Third, prior examples of mechanochemically induced changes in macroscopic physical properties involve either activation in solution (*8, 19*), irreversible plastic deformation (*20*), and/or the presence of reagents beyond the initial network (*19, 21*). Mechanophore designs offer an increasing range of responses (*22*), and the chemical changes that accompany reactive chain extension might be designed to produce additional, desirable responses.

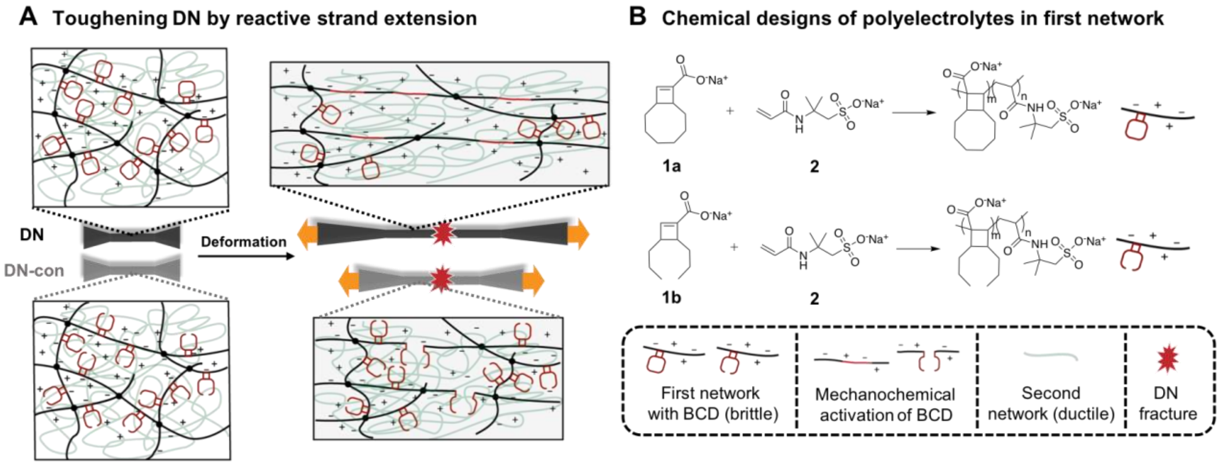

Fig. 1. The reactive strand extension (RSE) concept in double network hydrogels (strand scission events are not shown). (A) Schematic of double networks with RSE and analogous controls. (B) Chemical structures of the first network co-polymer strands employed in this work.

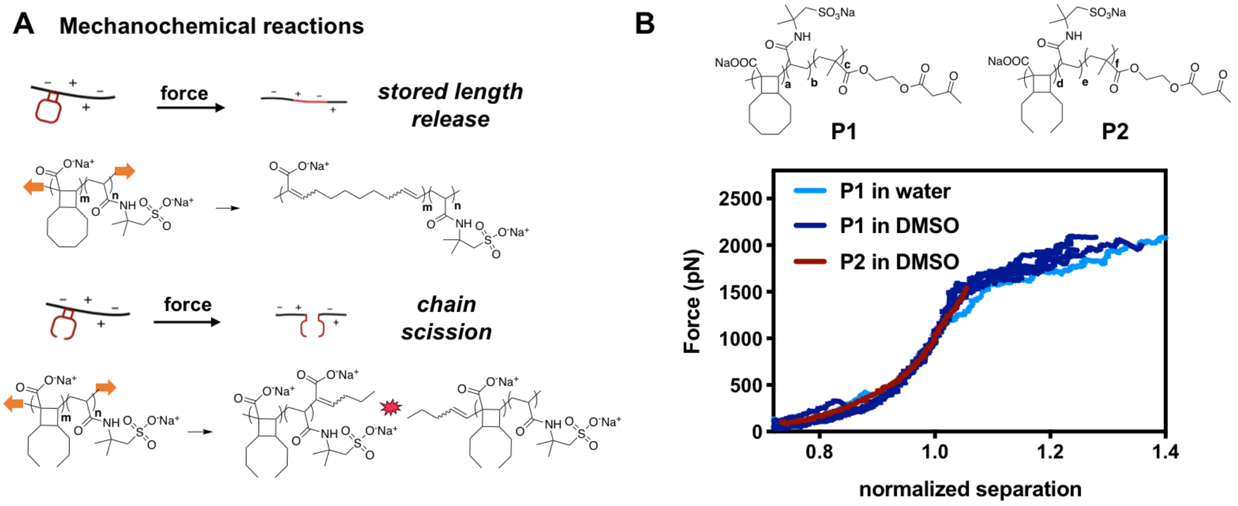

Fig. 2. Mechanochemical reactions driving RSE. (A) Mechanically coupled [2+2] cycloreversion leads to chain extension in [6.2.0]bicyclodecane mechanophores and to chain scission in analogous acyclic cyclobutane mechanophores. (B) Representative single molecule force-extension curves of linear RSE co-polymer **P1** in water and DMSO, and control co-polymer **P2** in DMSO.

Table 1. Young's modulus (*E*), nominal strain, nominal stress, and input energy density at break (ε_b, σ_b, and W_b, respectively) of unnotched films in unconstrained uniaxial tension, and crack propagation strain ($\boldsymbol{\varepsilon_p}$) and tearing energy (*T*) of films in a single-edge notched geometry. Tearing energy of PAAm gel is listed as reported (*23*).

	E (kPa)	ε_b	σ_b (MPa)	W_b (MJ m^{-3})	ε_p	T (J m^{-2})
DN1	288 ± 4	10.0	0.92	6.4	2.3	2840 ± 103
DN1-con	290 ± 8	4.9	0.61	2.3	1.7	1419 ± 52
DN2	243 ± 5	7.0	0.64	2.6	1.3	554 ± 40
DN2-con	249 ± 13	4.7	0.54	1.6	0.8	276 ± 10
PAAm	57 ± 6	5.0	0.18	0.4	/	~100

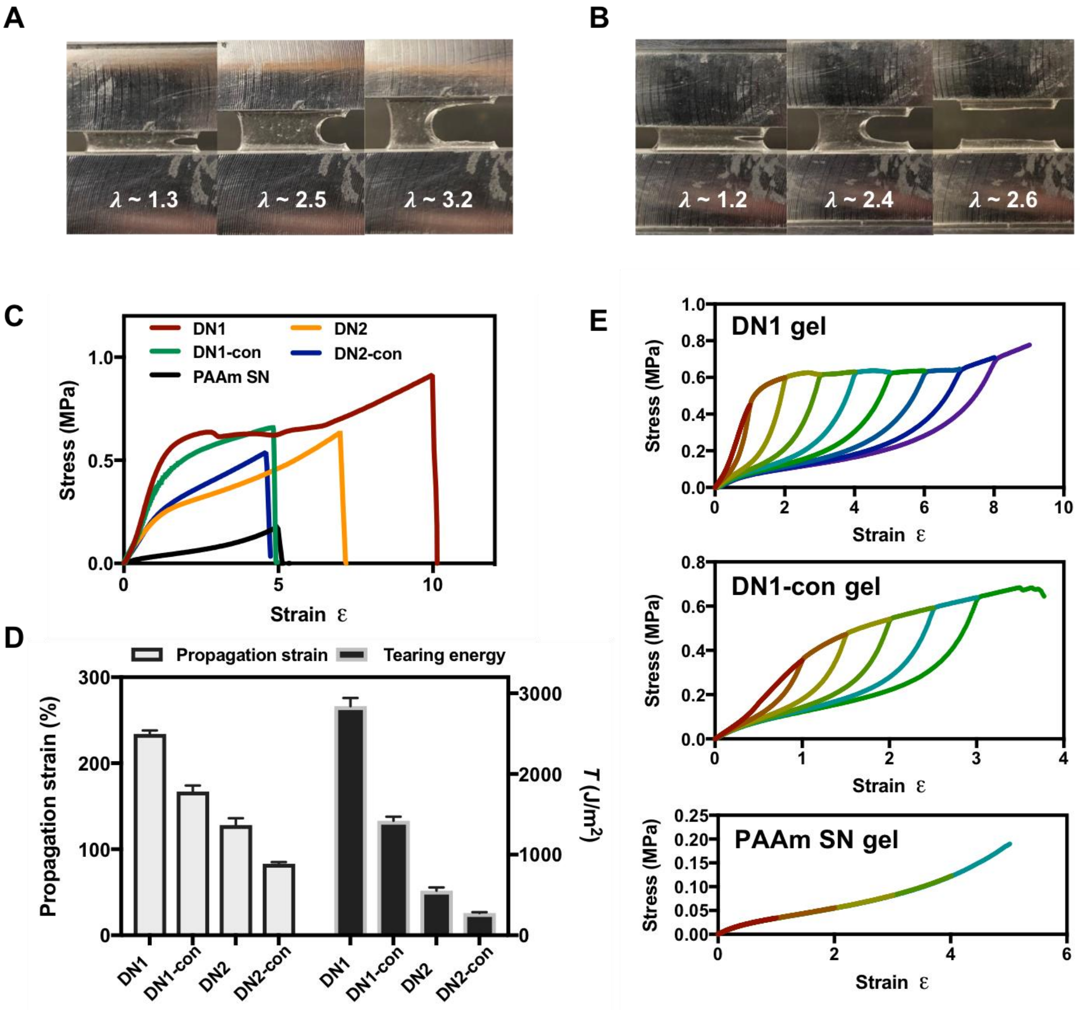

Fig. 3. Response of DNs to uniaxial tension. (A) Single-edge notched **DN1** at stretch ratios λ (mm/mm) of 1.3, 2.5, and 3.2. (B) Single-edge notched **DN1-con** at stretch ratios (mm/mm) of 1.2, 2.4, and 2.6. (C) Representative stress-strain curves (pure shear, 2 mm thick films) of unnotched DNs and a single PAAm network prepared identically to the second network of the DNs. (D) Propagation strain and tear energy of DNs. (E) Hysteresis in cyclic loading/unloading of **DN1**, **DN1-con**, and a single PAAm network prepared identically to the second network of the DNs. Note that the scales of the strain axes differ for the three loading/unloading curves.

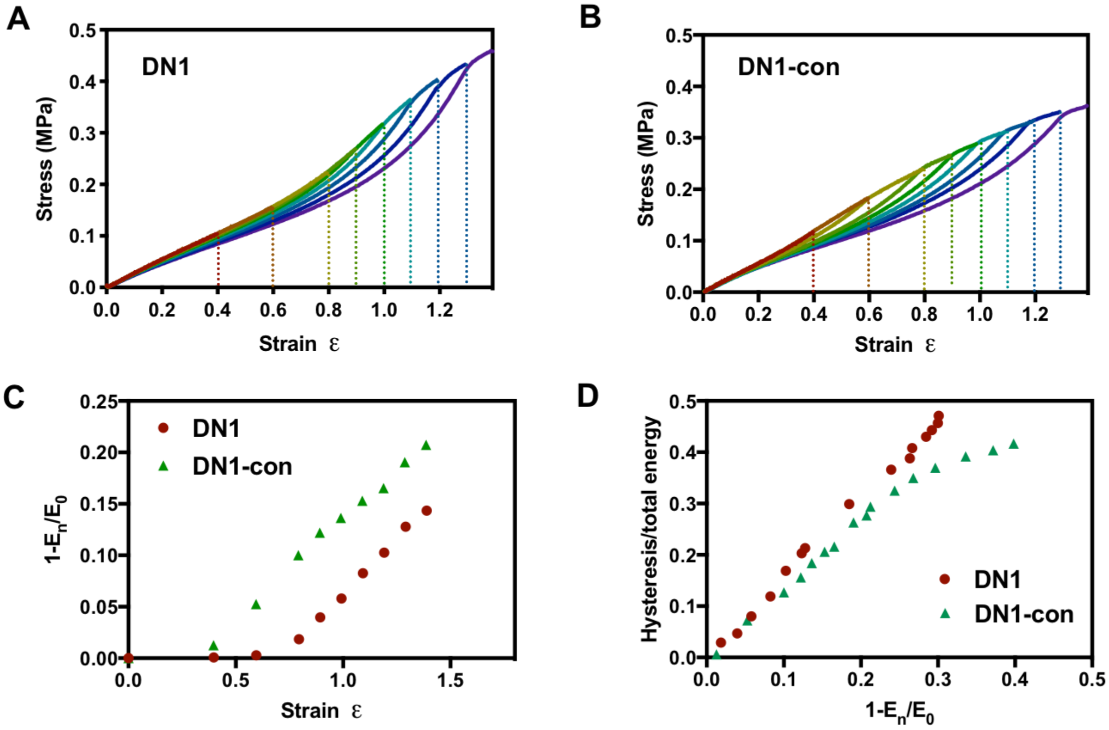

Fig. 4. Hysteresis analysis of DN1 and DN1-con. Cyclic loading/unloading of **DN1 (**A), and **DN1-con** (B) in small strain range; (C) Fractional loss of Young's modulus of **DN1** and **DN1-con** as a function of strain; (D) Fractional hysteresis as a function of fractional loss in modulus for **DN1** and **DN1-con**. 5

References and Notes:

1. M. M. Caruso *et al.*, Mechanically-induced chemical changes in polymeric materials. *Chemical Reviews* **109**, 5755-5798 (2009).
2. S. Lin *et al.*, Anti-fatigue-fracture hydrogels. *Science Advances* **5**, eaau8528 (2019).
3. X. Zhao, Multi-scale multi-mechanism design of tough hydrogels: building dissipation into stretchy networks. *Soft Matter* **10**, 672-687 (2014).
4. E. Ducrot, Y. Chen, M. Bulters, R. P. Sijbesma, C. Creton, Toughening elastomers with sacrificial bonds and watching them break. *Science* **344**, 186-189 (2014).
5. H. Lei *et al.*, Stretchable hydrogels with low hysteresis and anti-fatigue fracture based on polyprotein cross-linkers. *Nature Communications* **11**, 4032 (2020).
6. Z. Wang *et al.*, Stretchable materials of high toughness and low hysteresis. *Proceedings of the National Academy of Sciences* **116**, 5967 (2019).
7. S. Garcia-Manyes, A. E. M. Beedle, Steering chemical reactions with force. *Nature Reviews Chemistry* **1**, 0083 (2017).
8. Z. Chen *et al.*, Mechanochemical unzipping of insulating polyladderene to semiconducting polyacetylene. *Science* **357**, 475 (2017).
9. S. Wang, S. Panyukov, M. Rubinstein, S. L. Craig, Quantitative adjustment to the molecular energy parameter in the Lake–Thomas theory of polymer fracture energy. *Macromolecules* **52**, 2772-2777 (2019).
10. B. H. Bowser, C.-H. Ho, S. L. Craig, High mechanophore content, stress-relieving copolymers synthesized via RAFT Polymerization. *Macromolecules* **52**, 9032-9038 (2019).
11. Y. Tian *et al.*, A polymer with mechanochemically active hidden length. *Journal of the American Chemical Society* **142**, 18687-18697 (2020).
12. J. P. Gong, Why are double network hydrogels so tough? *Soft Matter* **6**, 2583-2590 (2010).
13. R. S. Rivlin, A. G. Thomas, Rupture of rubber. I. characteristic energy for tearing. *Journal of Polymer Science* **10**, 291-318 (1953).
14. T. Matsuda *et al.*, Yielding criteria of double network hydrogels. *Macromolecules* **49**, 1865-1872 (2016).
15. P. J. Flory, J. Rehner, Statistical mechanics of cross-linked polymer networks II. swelling. *The Journal of Chemical Physics* **11**, 521-526 (1943).
16. T. Nakajima, T. Kurokawa, S. Ahmed, W.-l. Wu, J. P. Gong, Characterization of internal fracture process of double network hydrogels under uniaxial elongation. *Soft Matter* **9**, 1955-1966 (2013).
17. T.-T. Mai, T. Matsuda, T. Nakajima, J. P. Gong, K. Urayama, Distinctive characteristics of internal fracture in tough double network hydrogels revealed by various modes of stretching. *Macromolecules* **51**, 5245-5257 (2018).
18. X. Wang, W. Hong, Pseudo-elasticity of a double network gel. *Soft Matter* **7**, 8576-8581 (2011).
19. Z. Wang, J. Ayarza, A. P. Esser-Kahn, Mechanically initiated bulk-scale free-radical polymerization. *Angewandte Chemie International Edition* **58**, 12023-12026 (2019).
20. A. L. B. Ramirez *et al.*, Mechanochemical strengthening of a synthetic polymer in response to typically destructive shear forces. *Nature Chemistry* **5**, 757 (2013).
21. T. Matsuda, R. Kawakami, R. Namba, T. Nakajima, J. P. Gong, Mechanoresponsive self-growing hydrogels inspired by muscle training. *Science* **363**, 504 (2019).

22. M. A. Ghanem *et al.*, The role of polymer mechanochemistry in responsive materials and additive manufacturing. *Nature Reviews Materials*, (2020).
23. J.-Y. Sun *et al.*, Highly stretchable and tough hydrogels. *Nature* **489**, 133 (2012).
24. J. Wang *et al.*, Inducing and quantifying forbidden reactivity with single-molecule polymer mechanochemistry. *Nature Chemistry* **7**, 323 (2015).
25. E. L. Florin *et al.*, Sensing specific molecular interactions with the atomic force microscope. *Biosensors and Bioelectronics* **10**, 895-901 (1995).
26. J. J. Lessard *et al.*, Block copolymer vitrimers. *Journal of the American Chemical Society* **142**, 283-289 (2020).
27. M.-A. B. Kruft, L. H. Koole, A convenient method to measure monomer reactivity ratios. Application to synthesis of polymeric biomaterials featuring intrinsic radiopacity. *Macromolecules* **29**, 5513-5519 (1996).
28. J. Undin, T. Illanes, A. Finne-Wistrand, A.-C. Albertsson, Random introduction of degradable linkages into functional vinyl polymers by radical ring-opening polymerization, tailored for soft tissue engineering. *Polymer Chemistry* **3**, 1260-1266 (2012).
29. T. B. Kouznetsova, J. Wang, S. L. Craig, Combined constant-force and constant-velocity single-molecule force spectroscopy of the conrotatory ring opening reaction of benzocyclobutene. *ChemPhysChem* **18**, 1486-1489 (2017).
30. S. B. Smith, Y. Cui, C. Bustamante, Overstretching B-DNA: the elastic response of individual double-stranded and single-stranded DNA molecules. *Science* **271**, 795 (1996).
31. I. M. Klein, C. C. Husic, D. P. Kovács, N. J. Choquette, M. J. Robb, Validation of the CoGEF method as a predictive tool for polymer mechanochemistry. *Journal of the American Chemical Society* **142**, 16364-16381 (2020).
32. T.-T. Mai, T. Matsuda, T. Nakajima, J. P. Gong, K. Urayama, Distinctive characteristics of internal fracture in tough double network hydrogels revealed by various modes of stretching. *Macromolecules* **51**, 5245-5257 (2018).

Acknowledgement:

We thank Y.J. Lin and P. Zhang for the assistance with DFT calculations, and M. Walters for the preparation of the experimental devices. **Funding**: This work was supported by the NSF Center for the Chemistry of Molecularly Optimized Networks (MONET), CHE-2116298, to J.A.J., J.A.K., B.D.O., M.R., and S.L.C. This work was partially supported by JSPS KAKENHI grant (JP17H06144 and JP21K14676) to J. P. G. **Author contributions:** Z.W., B.H.B. and S.L.C. conceived the concept. Z.W., T.O., H.K.B., T.M., S.W., J.A.J., J.A.K., B.D.O., J.P.G., M.R., and S.L.C designed the experiments. Z.W., X.J.Z., T.B.K., S.A.R. performed experiments and analyzed the data. Z.W., J.A.J., J.A.K., B.D.O., J.P.G., M.R., and S.L.C wrote the manuscript. **Competing interests:** T.M. is also affiliated with DSM Engineering Materials, Royal DSM, 6160 BB Geleen, The Netherlands. Z.W. is also affiliated with Lawrence Berkeley National Lab, Molecular Foundry, 67 Cyclotron Rd, Berkeley, CA 94720. **Data and materials availability:** All data are available in the manuscript or the supplementary materials.

Supplementary Materials

Materials and Methods
Supplementary Text
Figs. S1 to S11
Tables S1 to S4
Movies S1 to S2
References (24-32)